INSTITUTE OF PHYSICS PUBLISHING JOURNAL OF PHYSICS B: ATOMIC, MOLECULAR AND OPTICAL PHYSICS

J. Phys. B: At. Mol. Opt. Phys. **34** (2001) 1019–1038 www.iop.org/Journals/jb PII: S0953-4075(01)17555-3

Elastic electron scattering from C_6H_6 and C_6F_6

H Cho[1,3], R J Gulley[1], K Sunohara[2], M Kitajima[2], L J Uhlmann[1], H Tanaka[2] and S J Buckman[1]

[1] Atomic and Molecular Physics Laboratories, Research School of Physical Sciences and Engineering, Australian National University, Canberra, ACT 0200, Australia
[2] Department of Physics, Sophia University, Tokyo 102-8554, Japan

Received 28 September 2000

Abstract

We present absolute measurements of differential elastic electron scattering cross sections from benzene (C_6H_6) and hexafluorobenzene (C_6F_6). The measurements have been performed in our two laboratories on different crossed-beam apparatuses for scattering angles between 10° and 130°: C_6H_6 at the Australian National University in the energy range from 1.1 to 40 eV, and C_6F_6 at Sophia University from 1.5 to 100 eV. The cross sections for both molecules, which are characterized by strong forward-angle scattering and large-angle oscillations, are favourably compared with recent theoretical calculations.

1. Introduction

Considering its fundamental importance as the simplest aromatic hydrocarbon it is somewhat surprising that studies concerning the scattering of electrons from benzene are not particularly numerous. Indeed, to date, with the exception of the recent work from our own laboratory (Gulley and Buckman 1999), there have been no absolute differential scattering determinations for this molecule. Most of the previous experimental studies on electron–benzene scattering have been concerned with measurements of the total cross section (TCS) or with the energy dependence of various vibrational excitation modes, the latter studies mainly being focused on resonant effects below 10 eV. A similar situation applies for hexafluorobenzene with the only previous studies being mainly concerned with observing features in electron attachment studies. Both benzene and hexafluorobenzene are non-polar molecules but they do have extremely large polarizabilities (~ 70 and 65 au, respectively) and so one might expect their low-energy electron scattering cross sections to be dominated by polarization effects.

The first experimental work on electron–benzene interactions was reported by Holst and Holtsmark (1931), who measured the TCS at impact energies between 0.5 and 25 eV. More recently Sueoka (1988), Mozejko *et al* (1996) and Gulley *et al* (1998) have reported electron-impact TCS measurements over different energy regions: Sueoka (1988) measured the TCS for 0.7–400 eV positrons and 1.0–400 eV electrons, Mozejko *et al* (1996) measured the TCS from 0.6 eV to 3.5 keV, whilst Gulley *et al* (1998) concentrated on the very low energy (35 meV

[3] Permanent address: Physics Department, Chungnam National University, Taejon, South Korea.

0953-4075/01/061019+20$30.00

to 2 eV) region. The only absolute differential measurements to date, those of Gulley and Buckman (1999), were reported for elastic scattering at energies of 8.5 and 20 eV. To the best of our knowledge, the only published experimental or theoretical determinations for electron scattering from C_6F_6 are the absolute total cross section measurements of Kasperski *et al* (1997) for the energy range 0.6–250 eV, determined by employing the transmission method. The resulting cross section shows a relatively high magnitude (> 28 Å^2) throughout this energy range and exhibits a very broad peak stretching from 10 to 100 eV with some weak features, near 9.5 and 15 eV, superimposed on the peak.

Many experimental investigations of vibrational excitation and resonance effects for benzene at energies below about 10 eV have been reported. Schulz and collaborators (Sanche and Schulz 1973, Nenner and Schulz 1975, Azria and Schulz 1975, Wong and Schulz 1975) have studied benzene as part of their pioneering research activities on resonances. Mather and Hasted (1976) detected 22 resonances in the electron transmission spectrum of benzene in the energy range 0.5–11 eV. Burrow *et al* (1987) determined the vertical electron affinities and characterized the temporary anion state of a series of hydrocarbons including benzene, utilizing electron transmission spectroscopy. Allan (1989) has comprehensively reviewed the studies of resonances in benzene, along with many other species. Gallup (1993) provided symmetry selection rules for vibrational excitation by resonant electron impact based on a symmetry analysis of the contributions to the transition operator from vibronic coupling. In the main, experimental investigations of electron interactions with hexafluorobenzene have been concerned with the formation of negative ions (Marawar *et al* 1988, Christophorou and Datskos 1995, Weik and Illenberger 1995 and references therein).

On the theoretical side, efforts have also been limited, no doubt due to the complexity of calculations for such molecules. Gianturco and Lucchese (1998) have examined one-electron resonances arising in electron scattering processes from benzene using a parameter-free, exact-static-exchange plus correlation-polarization potential. They carried out calculations over a broad range of collision energies from about 0.001 eV up to about 30 eV. Bettega *et al* (2000) presented elastic cross sections obtained from *ab initio* calculations employing the Schwinger multichannel method within both the static-exchange and static-exchange-polarization approximations at selected energies between 2.23 and 30 eV. For hexafluorobenzene there have been two recent, unpublished calculations, both using the Schwinger variational technique (Natalense and Lucchese 2001, Winstead *et al* 1999). Natalense and Lucchese employed the polyatomic Schwinger variational method with Padé corrections, which takes advantage of the molecular symmetry to calculate elastic cross sections from 0.1 to 200 eV and the positions and widths of the resonances. They found that the presence of the fluorine atoms makes the one-electron resonances in the $e^- + C_6F_6$ scattering problem much narrower than the corresponding resonances in the $e^- + C_6H_6$ case and shifts them to higher energy. The presence of the fluorine atoms also introduces new resonances, making the C_6F_6 cross sections appear more highly structured.

In this paper, we have extended our previous absolute measurements of the differential cross section for elastic scattering on benzene (Gulley and Buckman 1999) to both higher and lower energies, in particular to the energy regions of the two low-energy shape resonances near 1 and 5 eV. In addition, we report the first absolute differential cross sections for elastic scattering on hexafluorobenzene. The measurements have been undertaken in our two laboratories on different experimental apparatuses: the benzene experiments at the Australian National University and hexafluorobenzene experiments at Sophia University. The measurements reported are the elastic differential cross sections (DCS) between 1.1 and 40 eV for benzene and DCS between 1.5 and 100 eV for hexafluorobenzene. Also reported are the energy dependence (excitation function) for the elastic scattering from benzene over two

energy regions, one near the 1.1 eV shape resonance and the other between 4 and 10 eV, the latter covering the region of influence of two broad shape resonances. A brief discussion of the experimental details is given in section 2, the results for both gases are presented and compared with theory in section 3 and we draw some conclusions in section 4.

2. Experimental considerations

The experimental measurements were carried out using two crossed-beam electron spectrometers, one located at the Australian National University (ANU) and the other at Sophia University, Japan (SU). Both spectrometers have been described in considerable detail previously (ANU, Brunger *et al* 1990, Gulley *et al* 1994; SU, Tanaka *et al* 1988). In a previous report (Kitajima *et al* 2000) we used these two apparatuses to compare measurements of the elastic differential cross sections from the same target gas, N_2O, and this paper contains a detailed discussion and comparison of the principal similarities and differences between the two experimental systems and between the experimental practices that are applied. Therefore, those details will not be repeated here.

The absolute electron energy scale is calibrated by observing either the position of the second quasi-vibrational resonance peak of the N_2^- $^2\Pi_g$ resonance at an energy of 2.198 eV for a scattering angle of 60° (Rohr 1977) or the position of the He^- $1s2s^2$ ^2S resonance at 19.367 eV (Brunt *et al* 1977). In both laboratories, the absolute cross sections at each energy and scattering angle were determined by use of the relative flow technique (Srivastava *et al* 1975, Nickel *et al* 1989). This technique relies on measurements of the ratio of scattered electron intensities for the gas of interest relative to that for a standard gas. The commonly used standard cross section is that of helium. For the present measurements, we have used the elastic differential cross sections of Nesbet (1979) at energies below 20 eV. At higher energies we have used the helium elastic scattering cross sections measured in this laboratory by Brunger *et al* (1992) or the recommended helium cross section set of Boesten and Tanaka (1992). In both laboratories the target gas was obtained from the saturated vapour above a liquid sample contained in a glass finger attached to the gas handling system. The vapour pressure above the liquid sample at 20°C was 78 Torr for C_6H_6 and 322 Torr for C_6F_6. To determine the gas flow conditions for each gas (see Kitajima *et al* (2000) for details) we have used hard-sphere diameters of 2.19, 5.3 and 10 Å for He, C_6H_6 and C_6F_6, respectively.

3. Results and discussion

3.1. Elastic differential cross sections for C_6H_6

Low-energy electron scattering from benzene is dominated by several negative-ion resonances, the most heavily studied of which are at 1.1 and 4.8 eV and are believed to be $^2E_{2u}$ and $^2B_{2g}$ shape resonances (Allan 1989) arising as a result of the temporary capture of an incident electron into $\pi^*(e_{2u})$ and $\pi^*(b_{2g})$ orbitals, respectively. The lowest-energy resonance has been of particular interest as high-resolution studies have shown a series of sharp, quasi-vibrational features (e.g. Burrow *et al* 1987, Gulley *et al* 1998). In this paper we have measured several elastic scattering excitation functions to determine the positions and angular behaviour of these resonances and these measurements are shown in figures 1 and 2. Figure 1 shows the energy dependence of the absolute elastic scattering cross section in the region of the $^2E_{2u}$ resonance at scattering angles of 60°, 90° and 120°. The dominant feature is the first vibrational peak at 1.1 eV but several, higher-energy peaks are also observed. The energy dependences at 60° and 120° are very similar, although there are slight differences in the resonance profiles, whilst at 90° none

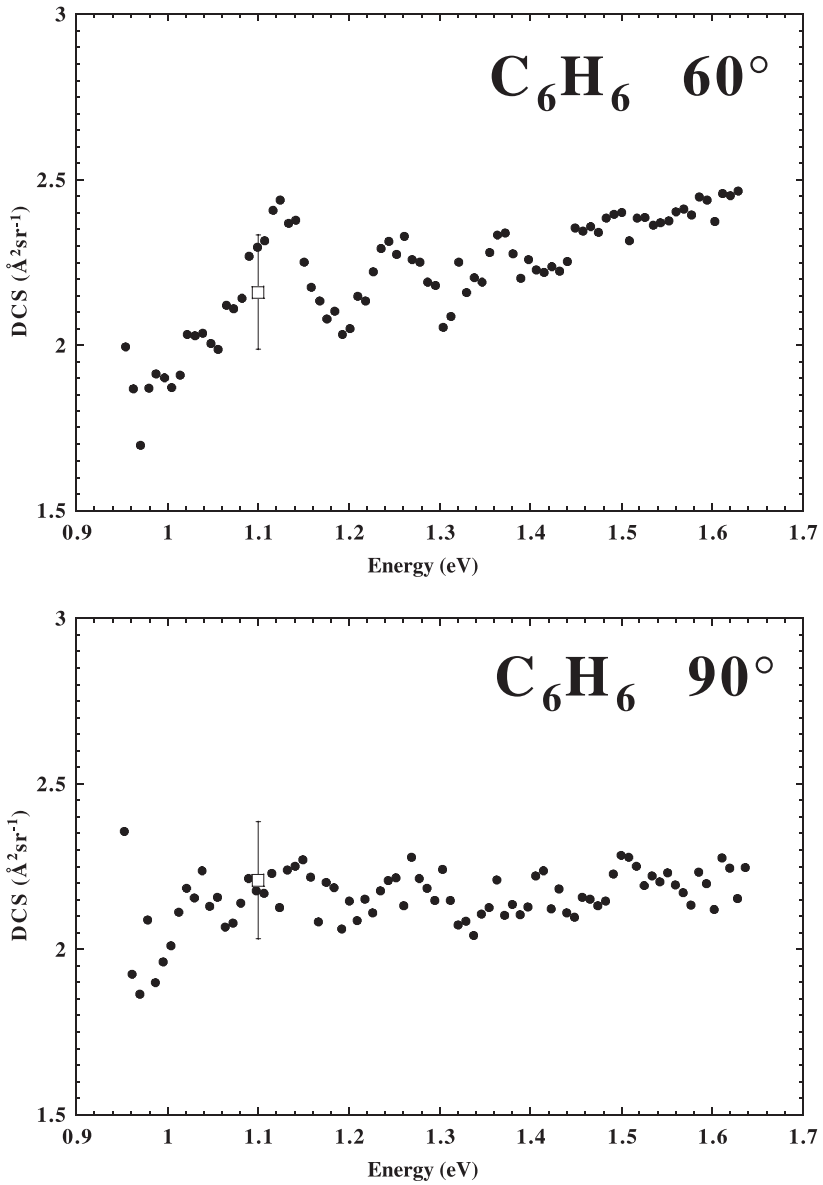

Figure 1. Elastic excitation function in the region of the $^2E_{2u}$ resonance at scattering angles of 60°, 90° and 120°: ●, present excitation function; □, present DCS.

of the resonance features are strongly present, consistent with the proposition (Bardsley and Read 1968) that this resonance decays via an f-wave electron. Figure 2 shows a similar series of measurements at higher energies (4–10 eV) where two broad resonance features are visible. The first is the '4.8 eV resonance', which we actually find (e.g. in the spectrum at 90° where it manifests as a peak) to be at an energy of 4.94 eV. This was determined by careful calibration against the quasi-vibrational resonance features in the $^2\Pi$ resonance in N_2. The other structure that we have observed is at around 8 eV. In addition we have searched, at energies near 21 eV,

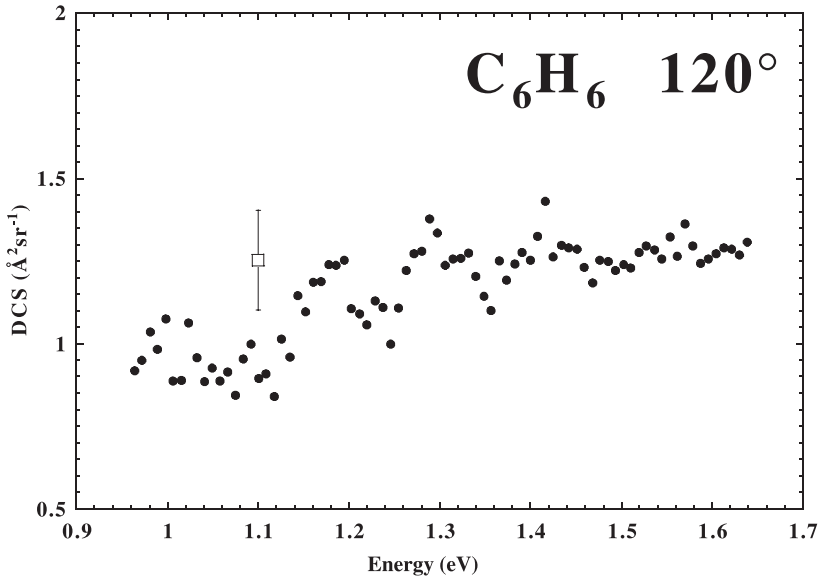

Figure 1. Continued.

for structure which may be associated with a resonance postulated by Gianturco and Lucchese (1998). There was no evidence of any such structure in the elastic scattering channel.

The elastic differential scattering measurements for C_6H_6 have been carried out at 13 different energies in the range from 1.1 to 40 eV. These data are presented in table 1 and examples of the DCS and comparisons with theory, where available, are provided in figures 3 and 4. The uncertainties in the DCS measurements, as shown in the table, are typically in the range of 8–12%. They arise from a combination (in quadrature) of the statistical uncertainties together with those arising from measurements of experimental parameters such as electron beam current, gas pressure and determination of relative flow rates.

As we have seen above, near 1.1 eV, the $^2E_{2u}$ resonance has been shown to demonstrate significant quasi-vibrational structure, indicating that the lifetime of the temporary anion is at least comparable to the vibrational period, and it has a significant effect on the scattering cross section (see, e.g., Gulley *et al* 1998). The DCS measured at the position of the first and strongest peak in the excitation function near 1.1 eV is shown in figure 3(*a*). There is a deep minima in the cross section at around 40°, and apparently another at an angle greater than 130°, and there is a broad maximum at about 75°. As discussed above, the $^2E_{2u}$ resonance is expected to autodetach an f-wave electron and this is consistent with minima near 40° and ∼140°, as well as at 90°. Given that there is significant non-resonant or direct elastic scattering at this energy, it is perhaps not surprising that the angular distribution is not purely f-wave in character. We also show in figure 3(*a*) the results of the parameter-free, exact-static-exchange plus correlation-polarization potential (SECP) calculation of Gianturco and Lucchese (1998), and the Schwinger multichannel (SMC) method calculation of Bettega *et al* (2000) at the energies where they found the corresponding peak of the $^2E_{2u}$ resonance, 1.815 and 2.23 eV, respectively. Their theoretical determinations agree very well with each other, but are considerably larger in magnitude than the present experimental results.

At 2 eV (figure 3(*b*)) the first minima and mid-angle maximum have both moved to lower angles and the cross section is substantially larger. Comparison with the SECP calculation of

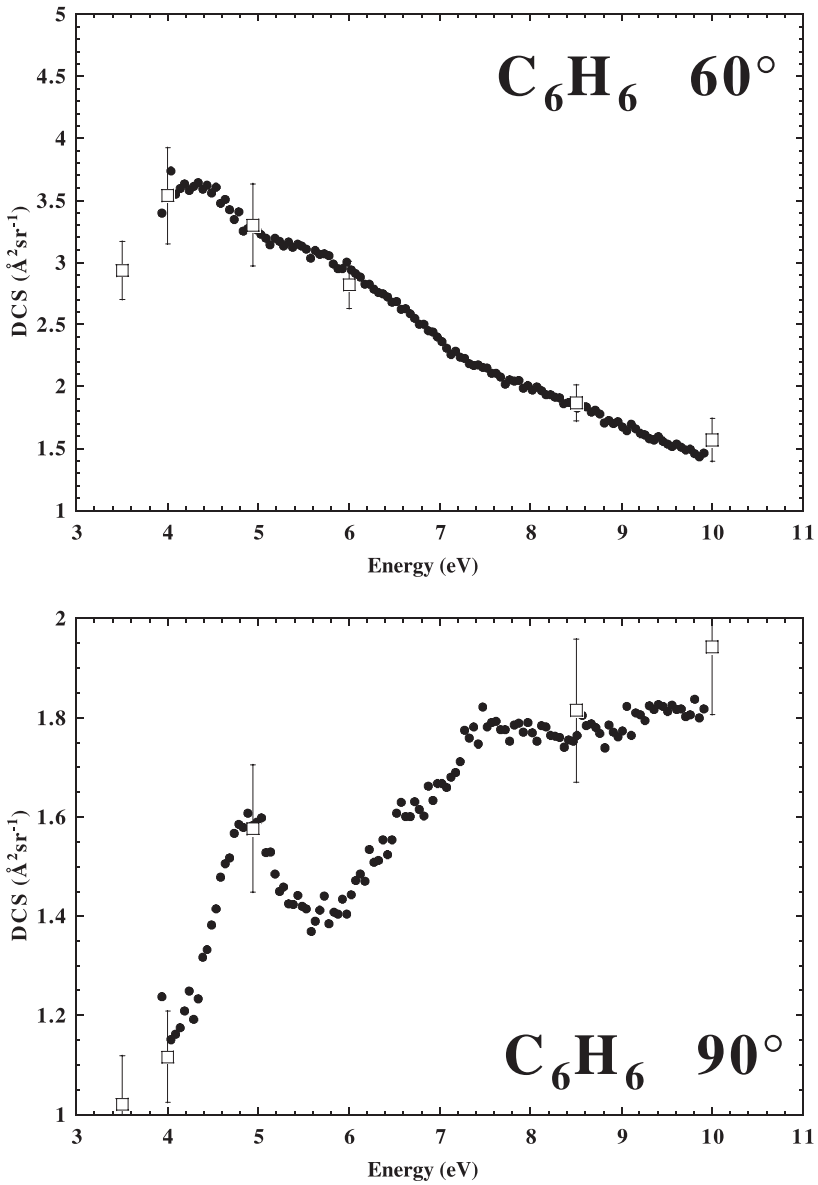

Figure 2. Elastic excitation function for the energy region 4–10 eV at scattering angles of 60°, 90° and 120°: ●, present excitation function; □, present DCS.

Gianturco and Lucchese (1998) at 2 eV does not reveal any similarity between experiment and theory. The SMC calculation of Bettega *et al* at 2.23 eV is again shown for this energy, but it must be noted that this result is at the energy where they found the $^2E_{2u}$ resonance.

At 3.0 eV (figure 3(*c*)), the maximum of the measured cross section now occurs at the smallest angle (20°) and a sharp minimum has developed in the DCS at forward angles ($\sim 30°$). In addition, the secondary maximum has moved in to about 50° and the large-angle minimum to an angle of about 110°. The calculation of Gianturco and Lucchese (1998) shows considerably

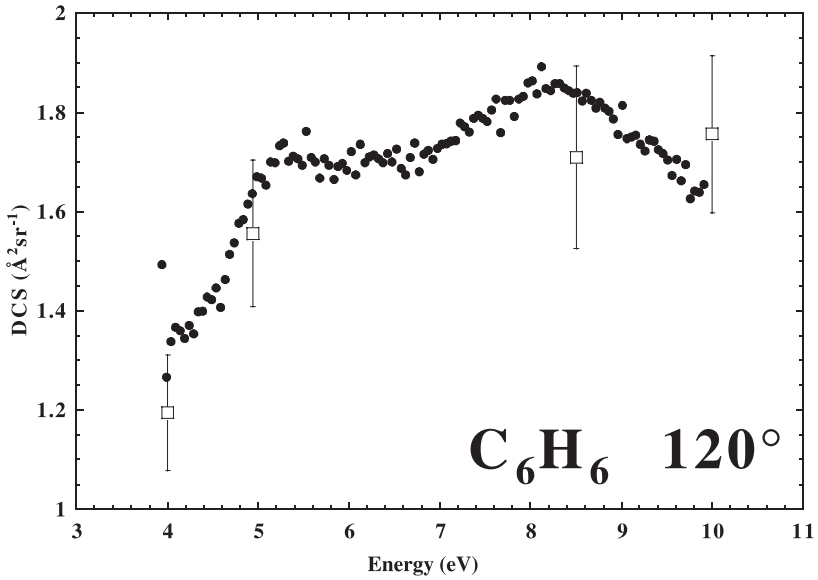

Figure 2. Continued.

better agreement with experiment at this energy, particularly for larger scattering angles. Whilst there are differences in the forward angle behaviour the calculation does show signs of a minimum in the cross section near 20°. At 4.0 eV (figure 3(*d*)) the forward scattering has again increased and the minimum at forward angles has disappeared, replaced by a slowly rising DCS between 50° and 20°. At 50° there is an abrupt change in slope of the DCS and a dramatic fall in the cross section occurs to the minimum at around 95°. Again, the calculation of Gianturco and Lucchese shows improved agreement with the present data at large scattering angles. We also measured the DCS at 3.5 eV, given the sudden change in the shape of the DCS between 3.0 and 4.0 eV, and it shows a rather similar result to that of 3.0 eV with the exception that the minimum at forward angles is somewhat shallower.

The DCS in figure 4(*a*) corresponds to a measurement at the peak of the $^2B_{2g}$ resonance feature, which we determine to be at an energy of 4.94 eV. The result at this energy is compared with the theoretical calculations of Gianturco and Lucchese, and Bettega *et al*. We note, however, that both of the calculated resonance energies are substantially higher than experiment: 7.44 and 8.3 eV, respectively. Therefore, in order to make the comparison meaningful, the present DCS at 4.94 eV is compared with the 7.44 eV result of Gianturco and Lucchese and the 8.3 eV result of Bettega *et al*. We also show the result of Gianturco and Lucchese at an energy of 5 eV for comparison. The overall agreement between the two calculations at the resonance energies is very similar, but the agreement with the experimental data is poor, especially at forward angles where the present result shows a flattening of the DCS. The substantial high angle structure in the theoretical calculations is not evident in the experimental DCS although some structure, indicative of higher ($l > 2$) partial-wave behaviour, is observed.

The DCS measurement at 6.0 eV (figure 4(*b*)) shows a substantially better level of agreement with theory. With the exception of a small structure at mid-angles, the calculated cross section is in excellent agreement with experiment. The DCS at 8.5 eV, the region of influence of a $^2E_{1u}$ shape resonance, has been discussed in a previous publication (Gulley and

Table 1. Differential cross sections for elastic electron scattering (in units of 10^{-16} cm^2 sr^{-1}) and total elastic and elastic momentum transfer cross sections, σ_i and σ_m, respectively (in units of 10^{-16} cm^2), from benzene. Figures in parentheses indicate estimated percentage uncertainties and the estimated uncertainty on the integral and momentum transfer cross sections is ±25%.

	Energy (eV)						
Angle (deg)	1.1	2.0	3.0	3.5	4.0	4.9	6.0
10	—	—	—	—	—	—	—
12	—	—	—	—	—	—	—
15	—	—	—	—	—	—	9.784(15)
20	1.929(8)	2.608(13)	4.644(8)	4.039(8)	7.460(8)	6.653(10)	11.585(9)
25	1.638(8)	2.354(11)	3.058(7)	2.472(9)	6.925(7)	7.455(8)	11.058(7)
30	1.358(9)	2.474(9)	2.538(9)	3.224(7)	6.503(7)	7.369(7)	9.016(7)
35	1.311(10)	2.631(8)	3.126(7)	3.448(7)	6.168(7)	6.697(7)	7.388(8)
40	1.297(10)	2.935(7)	3.493(7)	3.366(7)	5.939(7)	6.127(7)	6.304(7)
45	1.479(10)	2.983(8)	3.827(7)	3.409(7)	5.735(7)	5.614(7)	5.360(8)
50	1.573(7)	3.093(7)	3.779(7)	3.338(8)	5.426(7)	5.223(7)	4.527(7)
55	1.958(8)	3.124(7)	3.843(7)	3.120(7)	4.609(8)	4.401(7)	3.610(7)
60	2.160(8)	3.210(7)	3.676(10)	2.935(8)	3.538(11)	3.302(10)	2.820(7)
65	—	3.125(7)	3.262(12)	2.585(9)	2.840(10)	2.604(8)	2.197(7)
70	2.460(10)	2.949(7)	2.860(10)	2.141(10)	2.266(9)	2.145(7)	1.752(8)
75	—	2.742(7)	2.400(9)	1.759(10)	1.754(9)	1.742(8)	1.509(7)
80	2.461(8)	2.545(7)	2.036(8)	1.418(10)	1.398(9)	1.570(9)	1.406(7)
85	—	2.333(7)	1.698(8)	1.200(9)	1.195(9)	1.535(8)	1.410(7)
90	2.209(8)	2.076(7)	1.462(8)	1.020(10)	1.116(8)	1.577(8)	1.449(7)
95	—	1.872(7)	1.242(10)	0.906(9)	1.090(9)	1.595(9)	1.476(7)
100	1.932(14)	1.621(7)	1.100(8)	0.852(10)	1.116(9)	1.650(8)	1.486(7)
105	—	1.468(8)	1.015(8)	0.814(9)	1.130(10)	1.621(8)	1.503(7)
110	1.443(10)	1.283(7)	0.973(11)	0.824(8)	1.167(11)	1.613(10)	1.510(8)
115	—	1.162(7)	0.992(8)	0.826(8)	1.195(11)	1.573(10)	1.547(7)
120	1.253(12)	1.067(7)	1.027(11)	0.880(7)	1.194(10)	1.556(10)	1.609(7)
125	—	0.992(8)	1.187(8)	0.960(8)	1.264(11)	1.627(10)	1.613(7)
130	1.022(15)	0.923(7)	1.281(15)	1.126(10)	1.316(12)	1.711(11)	1.660(8)
σ_i	21.21	25.68	28.96	24.74	33.41	35.64	36.09
σ_m	19.12	19.96	21.49	18.95	22.10	25.37	24.05

	Energy (eV)					
Angle (deg)	8.5	10	15	20	30	40
10	—	—	—	—	69.845(10)	70.371(9)
12	—	—	—	49.437(12)	—	—
15	26.890(14)	35.446(20)	41.501(7)	34.819(9)	32.752(9)	26.330(12)
20	22.902(9)	26.168(13)	27.019(9)	18.460(9)	14.262(8)	9.268(9)
25	15.549(10)	16.384(13)	14.753(8)	9.762(8)	5.402(9)	3.475(8)
30	10.349(7)	10.849(8)	7.818(11)	4.390(10)	2.488(8)	1.594(8)
35	7.421(8)	6.900(8)	4.016(9)	2.121(8)	1.280(10)	1.149(8)
40	5.640(9)	4.791(12)	1.924(12)	1.103(8)	1.031(8)	0.956(8)
45	4.251(8)	3.447(9)	1.167(7)	0.707(9)	0.834(7)	0.993(8)
50	3.305(8)	2.520(13)	0.884(8)	0.665(9)	0.896(10)	0.926(9)
55	2.420(7)	1.899(10)	0.845(8)	0.751(8)	0.892(8)	0.763(8)
60	1.865(8)	1.569(11)	0.870(7)	0.826(8)	0.829(10)	0.603(8)
65	1.675(8)	1.447(8)	0.961(7)	0.873(8)	0.736(9)	0.472(9)
70	1.672(7)	1.550(8)	1.049(7)	0.903(8)	0.622(10)	0.379(10)
75	1.758(7)	1.759(7)	1.141(7)	0.866(8)	0.554(8)	0.344(8)
80	1.828(8)	1.890(9)	1.195(7)	0.834(8)	0.478(9)	0.336(11)

Table 1. Continued

	Energy (eV)					
Angle (deg)	8.5	10	15	20	30	40
85	1.824(7)	1.948(8)	1.199(7)	0.754(8)	0.447(9)	0.350(11)
90	1.815(8)	1.943(7)	1.186(7)	0.715(9)	0.431(10)	0.368(10)
95	1.703(7)	1.922(7)	1.108(7)	0.665(9)	0.464(9)	0.394(11)
100	1.679(7)	2.018(9)	1.036(7)	0.661(8)	0.490(13)	0.396(13)
105	1.702(7)	2.028(9)	0.949(7)	0.674(9)	0.557(12)	0.427(12)
110	1.720(8)	2.041(9)	0.924(7)	0.696(10)	0.599(12)	0.466(13)
115	1.749(9)	1.974(9)	0.906(8)	0.742(10)	0.638(12)	0.529(13)
120	1.710(11)	1.756(9)	0.963(8)	0.832(11)	0.687(11)	0.585(17)
125	1.590(10)	1.571(11)	1.091(8)	0.921(13)	0.755(13)	0.669(18)
130	1.442(12)	1.428(11)	1.295(9)	1.039(14)	0.919(16)	0.734(21)
σ_i	44.94	47.75	33.79	33.33	31.08	26.90
σ_m	23.88	24.29	14.95	15.06	11.66	9.19

Buckman 1999) and is not shown again. We note, however, that the more recent theoretical results of Bettega *et al* are very similar in magnitude and shape to that of Gianturco and Lucchese, and as such are also in excellent agreement with the experimental result at this energy.

At 10 eV (figure 4(*c*)) forward scattering is becoming dominant and some oscillatory behaviour is again observed in the DCS between 60° and 130°. The theoretical results of Bettega *et al* and Gianturco and Lucchese are almost identical at this energy apart from slight discrepancies in the extreme forward direction. Bettega *et al* have attributed these discrepancies to insufficient representation of higher partial waves in their calculation. The agreement at forward angles of the present data with both theoretical results is again excellent at this energy, and this level of agreement continues to be seen at all of the other higher energies measured, 15, 20, 30 and 40 eV. At higher angles, the experimental DCS does not show the same, strong oscillatory behaviour as is evident in the calculated cross sections, although the general features of the cross section are reasonably well reproduced by the calculation. Finally, in figure 4(*d*) we show the DCS at 40 eV where the forward scattering is seen to be extremely strong. The cross section drops sharply from around 70 Å^2 at 10° to a sharp shoulder at 40° and a broad minimum at around 80°, where the magnitude of the cross section is almost a factor of ten less than at a similar scattering angle at 10 eV. The theoretical calculation of Gianturco and Lucchese predicts the shape of the cross section rather well, including the small shoulder, but at backward angles it overestimates the cross section magnitude. Graphical representations of the present data at 15, 20 and 30 eV can be found in previous publications (Gulley and Buckman 1999, Bettega *et al* 2000) and they are not repeated here.

3.2. Elastic differential cross sections for C_6F_6

Since many hydrocarbons and their fluorinated and/or chlorinated derivatives are used in various applications, including plasma processing, the effects of fluorination and chlorination have been studied in a number of systems (Tanaka *et al* 1997, 1999, Natalense *et al* 1999, Karwasz *et al* 1999). It was demonstrated in these studies that when hydrogen atoms are replaced by fluorine or chlorine atoms, the increase in molecular size is generally matched by an increase in their differential and total cross sections for electron scattering. It was also

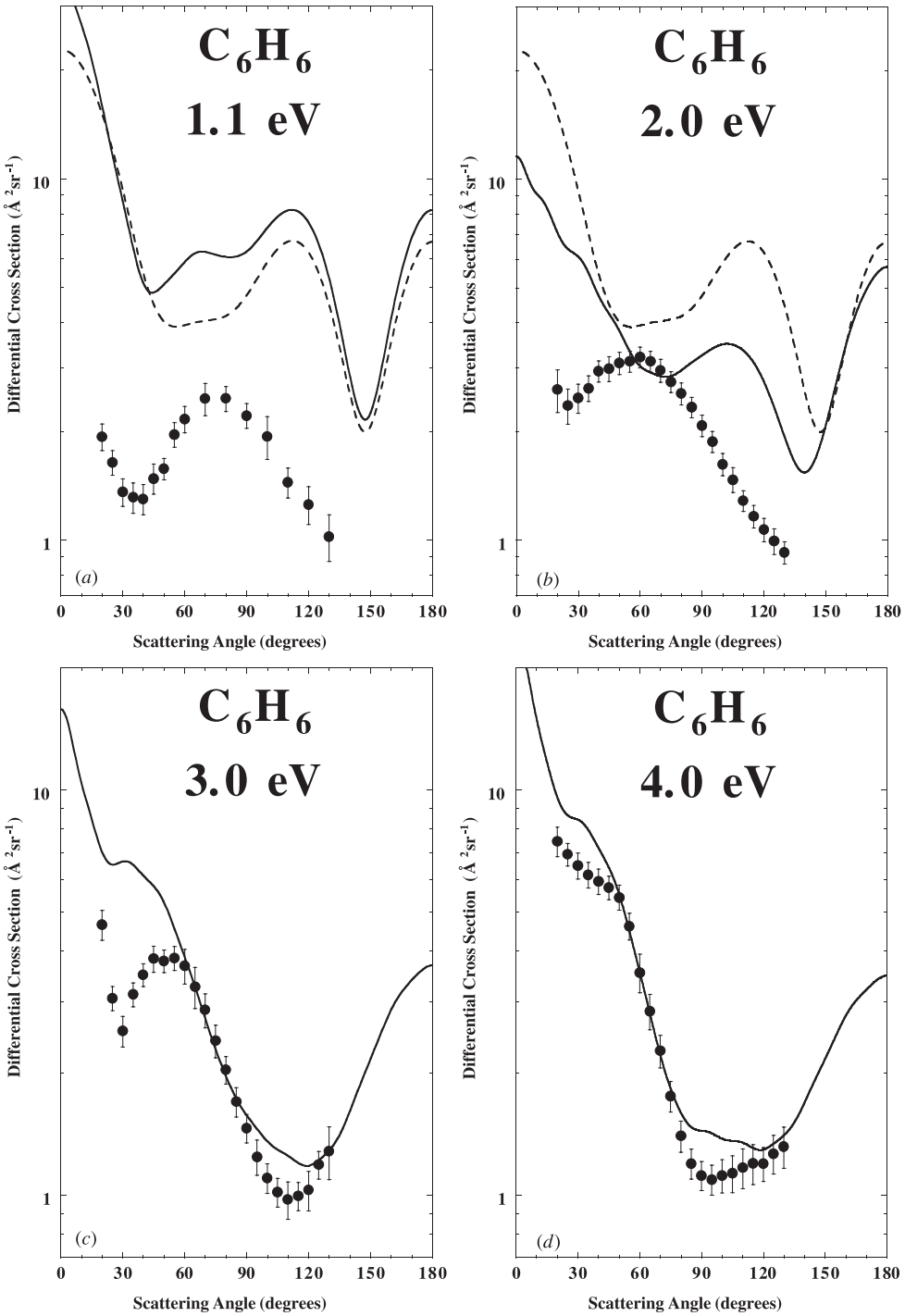

Figure 3. Absolute differential cross sections for elastic electron scattering from C_6H_6 at (*a*) 1.1 eV: ●, present data; ——, Gianturco and Lucchese (1998) at 1.815 eV; - - - -, Bettega *et al* (2000) at 2.23 eV; (*b*) 2.0 eV: ●, present data; ——, Gianturco and Lucchese (1998); - - - -, Bettega *et al* (2000) at 2.23 eV; (*c*) 3.0 eV: ●, present data; ——, Gianturco and Lucchese (1998); and (*d*) 4.0 eV: ●, present data; ——, Gianturco and Lucchese (1998).

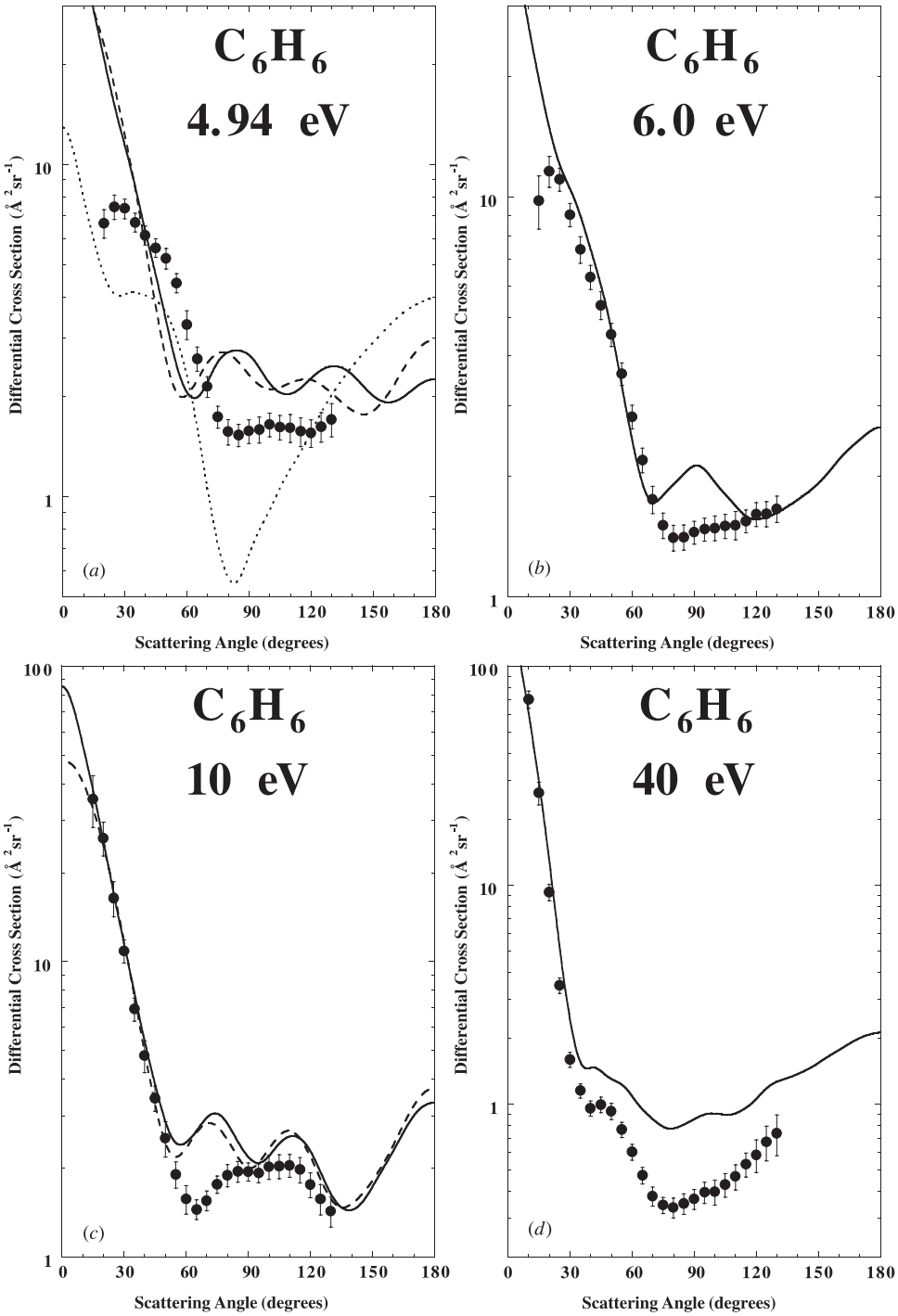

Figure 4. Absolute differential cross sections for elastic electron scattering from C_6H_6 at (*a*) 4.94 eV: ●, present data; ——, Gianturco and Lucchese (1998) at 7.44 eV: - - - -, Gianturco and Lucchese (1998) at 5 eV; – – –, Bettega *et al* (2000) at 8.3 eV; (*b*) 6.0 eV: ●, present data; ——, Gianturco and Lucchese (1998); (*c*) 10 eV: ●, present data; ——, Gianturco and Lucchese (1998); - - - -, Bettega *et al* (2000); and (*d*) 40 eV: ●, present data; ——, Gianturco and Lucchese (1998).

observed that the DCS for these fluorinated and chlorinated molecules generally exhibited more complex angular structure than the corresponding hydrocarbons.

The elastic differential cross sections for electron scattering from C_6F_6 have been measured at 10 different energies in the range from 1.5 to 100 eV. The data are presented in table 2 and some examples of the elastic DCS for C_6F_6 are given in figures 5 and 6. The absolute uncertainty in these measurements, as shown in the table, is estimated to be 15%. Where available, we have compared the experimental results with recent Schwinger variational calculations of Winstead *et al* (1999) and Natalense and Lucchese (2001). The unpublished results of Winstead *et al* are from preliminary calculations, which neglect polarization and using a fairly modest basis set. However, as we shall show, the agreement between the experimental and theoretical results is generally good and we have included these results for comparison with our experimental data. In figure 5 we see that the elastic DCS for C_6F_6 at energies below 10 eV show a very uniform pattern, with strong forward scattering and a broad cross section minimum in the range 70°–100°. This trend is in stark contrast to C_6H_6, where the low-energy DCS change quite abruptly over a very narrow energy range. However, we shall make some further comments about these differences in the next section.

At 1.5 eV (figure 5(*a*)), the agreement between experiment and the theoretical calculation of Winstead *et al* is reasonably good, especially at forward angles, even though the calculation does not predict the minimum in the cross section at 100°. At 3 eV (figure 5(*b*)), the comparison between experiment and theory is rather poor, with the calculation overestimating forward angle scattering and underestimating backward angle scattering. At 5 eV (figure 5(*c*)), we can compare the experimental results with the Schwinger variational calculations of Winstead *et al* (1999), and Natalense and Lucchese (2001). Both theoretical calculations overestimate the forward angle scattering. The calculation of Winstead *et al* predicts a minimum in the cross section but at a scattering angle of 110° as opposed to around 85° in the experimental results, whilst the calculation of Natalense and Lucchese shows a small maximum in the cross section at this angle. The agreement between experiment and theory is somewhat better at 8 eV (figure 5(*d*)) compared with the lower incident electron energies. The results of Natalense and Lucchese show excellent agreement with experiment in regard to the shape of the cross section, although the magnitude is around a factor of two higher over the majority of scattering angles. The results of Winstead *et al* show more structure in the DCS than was present in this calculation at 5 eV. However, comparison with the present data shows that the minima in the calculated cross section are again shifted (by around 30°) to higher scattering angles.

At higher incident electron energies (10–30 eV, figure 6), the experimental data and both theoretical results show good agreement, both in shape and overall magnitude. As we have seen in C_6H_6, the magnitude of the cross sections in this energy range are generally larger than at lower energies, particularly for forward angle scattering. The DCS at 10 eV (figure 6(*a*)) has increased in magnitude for scattering angles above 30° when compared with 8 eV. The calculation of Natalense and Lucchese shows excellent agreement with the shape of the experimental cross section, but again slightly overestimates the magnitude. The calculation of Winstead *et al* is much improved at this energy, showing excellent agreement with the experimental data, except for the small angular range of 90° to 120° where the calculation exhibits a local minimum. The present data at 15 eV (figure 6(*b*)) clearly display two minima with similar magnitudes, around 60° and 100°. These minima are predicted well by the calculation of Winstead *et al*. However, whilst the calculation of Natalense and Lucchese shows general agreement with the magnitude of the cross section, it does not show the same agreement with the shape, in contrast to lower incident energies. At 20 eV (figure 6(*c*)), the first minimum has shifted slightly in angle to 50°,

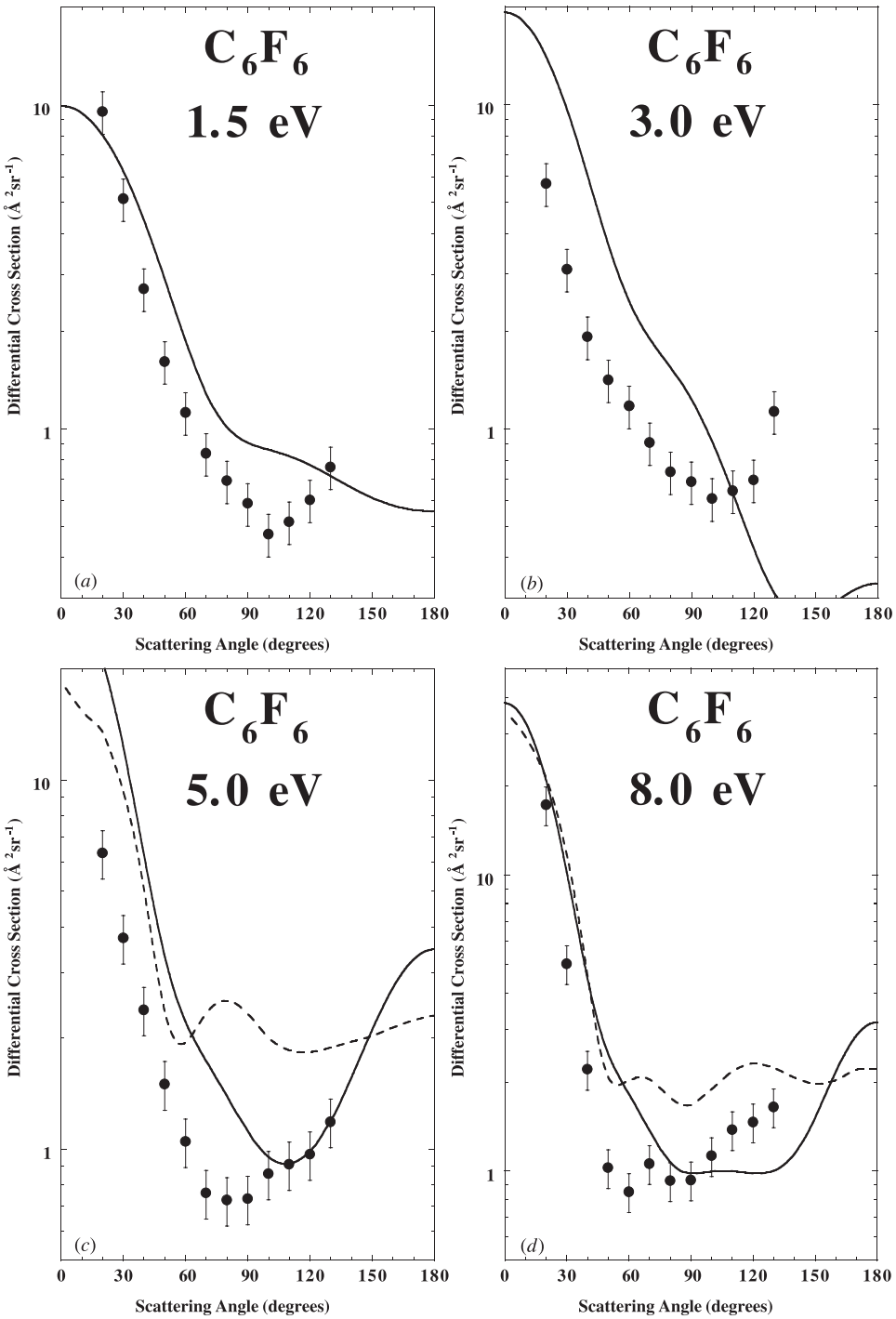

Figure 5. Absolute differential cross sections for elastic electron scattering from C_6F_6 at (*a*) 1.5 eV: ●, present data; ——, Winstead *et al* (1999); (*b*) 3.0 eV: ●, present data; ——, Winstead *et al* (1999); (*c*) 5.0 eV: ●, present data; ——, Winstead *et al* (1999); - - - -, Natalense and Lucchese (2001); and (*d*) 8.0 eV: ●, present data; ——, Winstead *et al* (1999); - - - -, Natalense and Lucchese (2001).

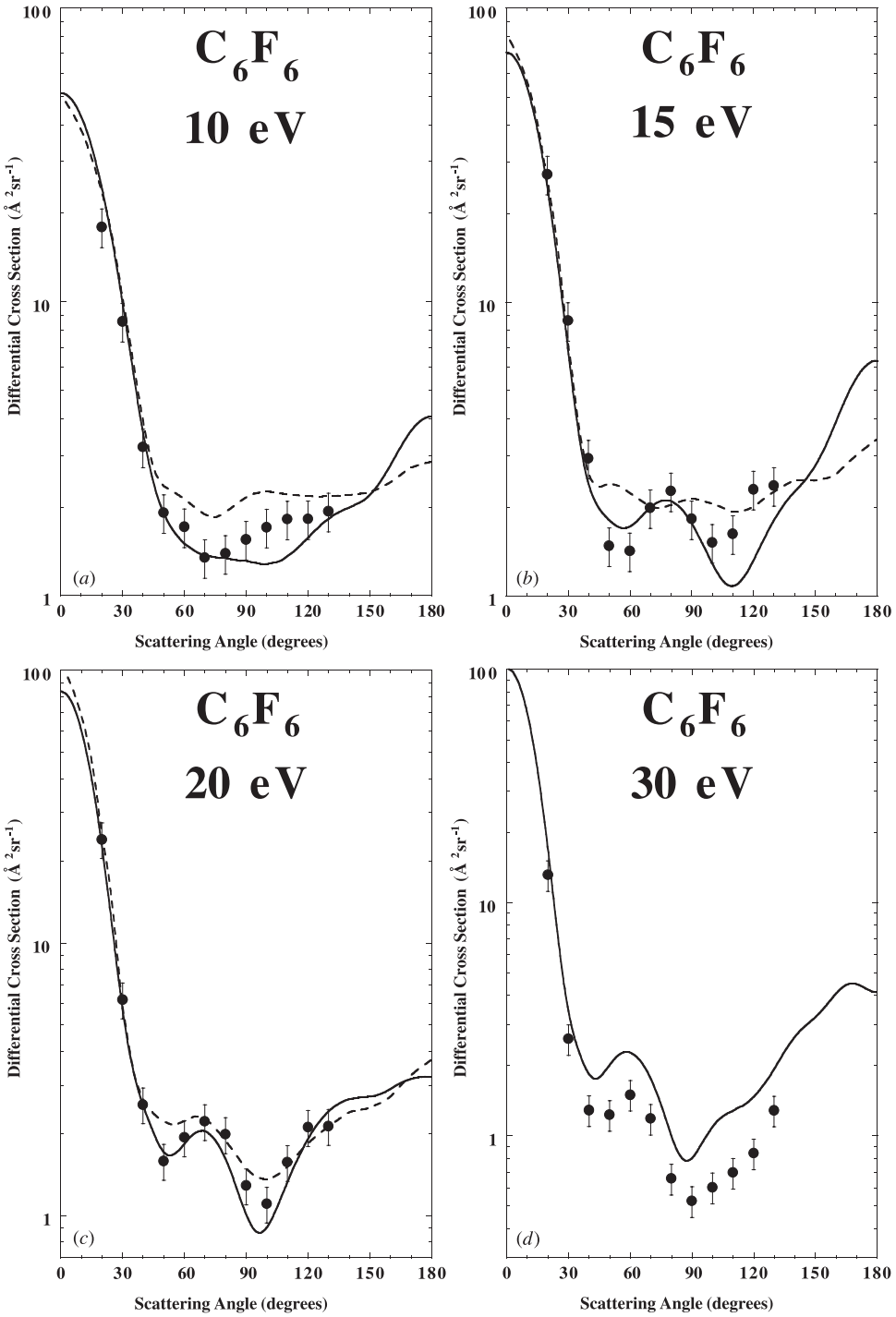

Figure 6. Absolute differential cross sections for elastic electron scattering from C_6F_6 at (*a*) 10 eV: ●, present data; ——, Winstead *et al* (1999); - - - -, Natalense and Lucchese (2001); (*b*) 15 eV: ●, present data; ——, Winstead *et al* (1999); - - - -, Natalense and Lucchese (2001); (*c*) 20 eV: ●, present data; ——, Winstead *et al* (1999); - - - -, Natalense and Lucchese (2001); and (*d*) 30 eV: ●, present data; ——, Winstead *et al* (1999).

Table 2. Differential cross sections for elastic electron scattering (in units of 10^{-16} cm^2 sr^{-1}) and total elastic and elastic momentum transfer cross sections, σ_i and σ_m, respectively (in units of 10^{-16} cm^2) from hexafluorobenzene. The estimated uncertainty in the data is 15%, whilst the uncertainty on the integral and momentum transfer cross sections is 25%.

	Energy (eV)						
Angle (deg)	1.5	3.0	5.0	8.0	10	15	20
20	9.534	5.695	6.330	17.31	17.99	27.23	23.96
30	5.130	3.103	3.731	5.023	8.583	8.649	6.193
40	2.706	1.917	2.382	2.208	3.201	2.941	2.553
50	1.612	1.412	1.498	1.024	1.915	1.480	1.585
60	1.123	1.174	1.047	0.851	1.713	1.422	1.932
70	0.840	0.904	0.760	1.059	1.346	1.993	2.217
80	0.690	0.736	0.727	0.927	1.391	2.276	1.984
90	0.588	0.685	0.733	0.931	1.554	1.828	1.288
100	0.472	0.608	0.856	1.125	1.708	1.519	1.104
110	0.515	0.643	0.908	1.378	1.820	1.628	1.570
120	0.602	0.694	0.967	1.463	1.824	2.308	2.108
130	0.762	1.129	1.185	1.646	1.938	2.371	2.128
σ_i	21.75	18.60	21.51	30.98	41.09	51.62	48.01
σ_m	11.49	14.25	16.54	18.50	24.40	29.93	26.35

	Energy (eV)		
Angle (deg)	30	60	100
20	13.14	6.583	2.594
30	2.601	2.374	1.918
40	1.290	2.065	1.095
50	1.230	1.416	0.418
60	1.502	0.658	0.464
70	1.185	0.386	0.379
80	0.655	0.428	0.218
90	0.525	0.425	0.179
100	0.602	0.367	0.189
110	0.695	0.364	0.217
120	0.841	0.493	0.319
130	1.286	0.779	0.402
σ_i	32.65	24.26	9.04
σ_m	16.86	11.58	5.63

whilst the magnitude of the second minimum at 100° has decreased. Both theoretical results show good agreement at this energy. At 30 eV (figure 6(*d*)), comparison with the only theoretical results of Winstead *et al* show excellent agreement in terms of the shape of the cross section. However, the calculated result is larger than the present data by a factor of ∼1.5. At even higher energies of 60 and 100 eV (not shown), the magnitude of forward angle scattering decreases and this is reflected in the magnitude of the total cross section at these energies. However, the DCSs still show structure at medium angles (40°–120°).

3.3. Total elastic and elastic momentum transfer cross sections for C_6H_6 and C_6F_6

The total elastic cross section σ_i and the elastic momentum transfer cross section σ_m have been evaluated from the present differential cross section results by extrapolating to forward and

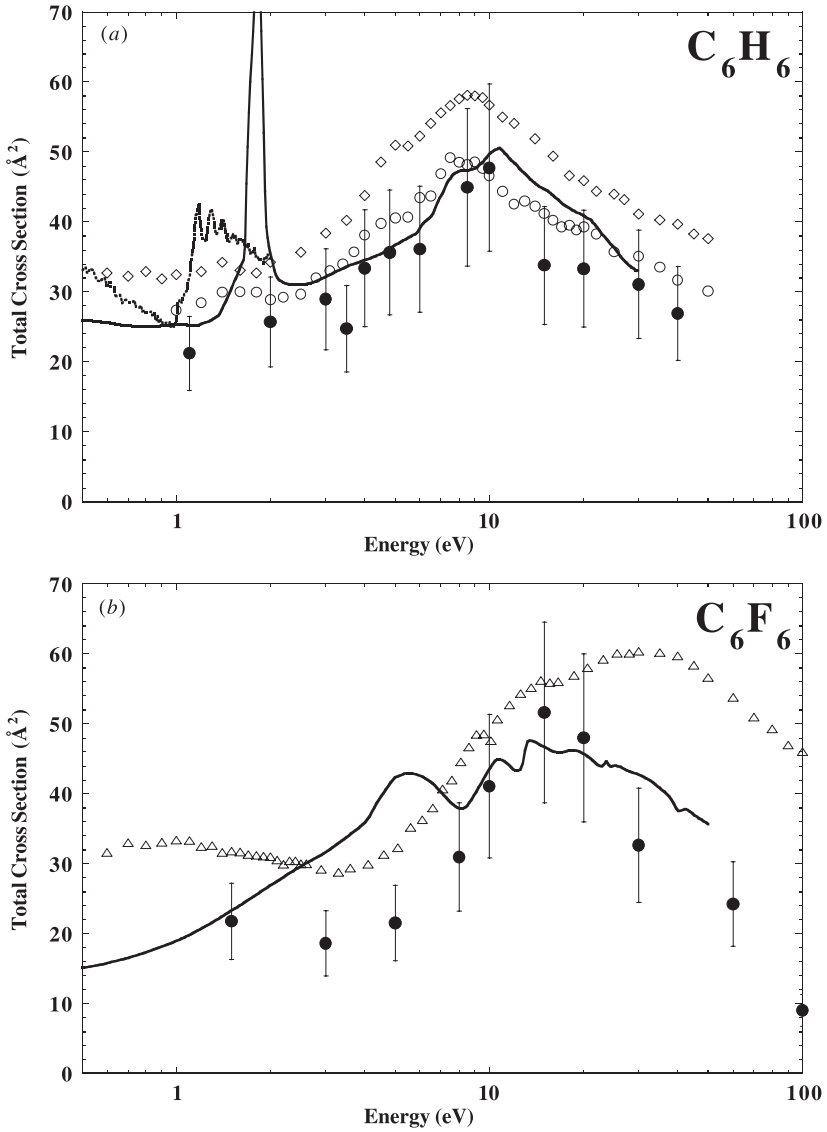

Figure 7. Integral elastic cross section for (*a*) C_6H_6: ●, present data; ——, Gianturco and Lucchese (1998); and (*b*) C_6F_6: ●, present data; ——, Winstead *et al* (1999). Also shown are the grand total cross sections for (*a*) C_6H_6: - - - -, Gulley *et al* (1998); ◇, Mozejko *et al* (1996); ○, Sueoka (1998); and (*b*) C_6F_6: (△) Kasperski *et al* (1997).

backward angles, and integrating the resultant cross sections. The values for these integral cross sections derived from this process are listed at the foot of each column in tables 1 and 2 for benzene and hexafluorobenzene, respectively. Where possible, the theoretical calculations have been used as a guide in the extrapolation process where agreement is good. However, where experiment and theory show substantial differences, particularly at low energies, the extrapolation has been largely done 'by eye'. The resulting uncertainties in these cross sections are estimated to be ±25%.

Figure 7(*a*) shows the elastic integral cross section for C_6H_6, where we compare with the elastic integral cross section result of Gianturco and Lucchese (1998), and the grand total cross section determinations of Gulley *et al* (1998), Mozejko *et al* (1996) and Sueoka (1998). It is noted that although the general character of the grand total cross sections is similar, the results of Mozejko *et al* are higher than the results of Sueoka by 10–20%. Mozejko *et al* have attributed this difference to a systematic error in the results of Sueoka due to the presence of their guiding magnetic field, leading to an uncertainty in the effective length of the interaction region. The most prominent feature in the total cross section is the enhancement at 8–9 eV, where the cross section of Mozejko *et al* peaks at a value of 58 Å^2. A similar enhancement has also been noted in the excitation functions for vibrational excitation of Azria and Schulz (1975) and Allan (1989). Allan assigned this structure to a $^2E_{1u}$ shape resonance, with capture of the electron into the $\sigma^*(e_{1u})$ orbital. This resonance is very broad and almost certainly overlaps the lower-energy $^2B_{2g}$ resonance at 4.9 eV, which is visible in the grand total cross sections as a weak shoulder. The very high-resolution studies of Gulley *et al* (1998) clearly show the enhancement of the total cross section due to the $^2E_{2u}$ shape resonance between 1 and 2 eV. The agreement between the present data and the theoretical results of Gianturco and Lucchese is generally good, within experimental errors for most incident electron energies, although the present results lie below the theoretical curve at all energies.

Figure 7(*b*) shows the elastic integral cross section for C_6F_6, where we compare with the elastic integral cross section of Winstead *et al* (1999) and the grand total cross section of Kasperski *et al* (1997). In the energy range between 5 and 100 eV, the total cross section increases rapidly as a function of energy from 28 Å^2 up to a value in excess of 55 Å^2 between 15 and 60 eV, peaking in the vicinity of 30 eV. Above 40 eV, the total cross section decreases constantly in magnitude down to a value of 46 Å^2 at 100 eV. At least two weak structures are observed on the low-energy side of this broad peak, one at around 9.5 eV and the other close to 14 eV. Both features have been attributed to core-excited temporary negative-ion resonance formation, with the resonance decomposing either through the re-emission of the additional electron or through dissociation leading to the formation of F^-, $C_5F_3^-$ and $C_6F_5^-$ ions (Kasperski *et al* 1997). Resonant structure has also been observed near 4.5 eV in transmission spectra and negative-ion yield curves, although this is not reflected in the DCS at 5 eV (figure 5(*c*)). The large magnitudes in this energy range for the total cross section are reflected in the elastic integral cross section values determined from the DCSs, with the largest value at an energy of 15 eV. The elastic integral cross sections at 30, 60 and 100 eV are clearly smaller in magnitude than the grand total cross section of Kasperski *et al*. The elastic cross section at 100 eV is 9 Å^2, a factor of five smaller in magnitude than the grand total cross section value of 46 Å^2. The differences in magnitude due to inelastic processes is most likely due to ionization, much like benzene where normalized electron-scattering ionization at 75 eV constitutes about one third of the grand total cross section (Mozejko *et al* 1996).

3.4. Comparison between the cross sections for C_6F_6 with those for C_6H_6

At low energies we can compare the differential cross sections for C_6H_6 at 1.1 and 2 eV with C_6F_6 at 1.5 eV (figure 8(*a*)). As mentioned previously, this is the region of the $^2E_{2u}$ resonance in C_6H_6. For C_6F_6, features below this energy range have been observed at around 0.45 eV in electron attachment studies and slightly below 0.8 eV in electron transmission experiments (Kasperski *et al* 1997) and these have been attributed to the formation of the temporary negative ion $C_6F_6^-$ with resonant capture of the incident electron into the π^* orbital. The DCS for C_6F_6 shows strong forward scattering with a value of 9.5 Å^2 at 20°, decreasing to a minimum of 0.47 Å^2 at 100°. In contrast, the differential cross sections for C_6H_6 show maxima around

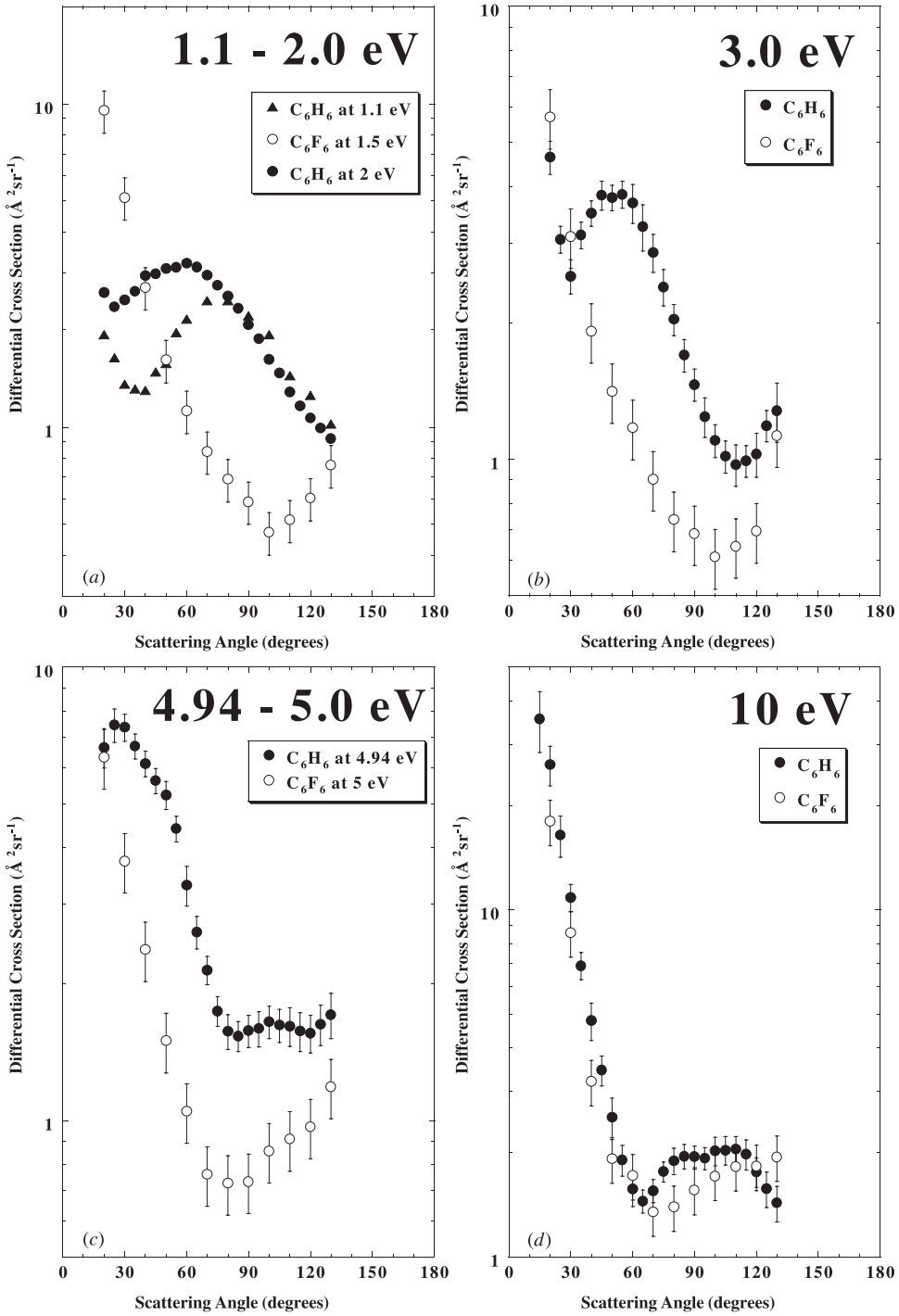

Figure 8. Comparison between the differential cross sections for (*a*) C_6H_6 at ▲, 1.1 eV and ●, 2.0 eV, and C_6F_6 at ○, 1.5 eV; (*b*) at 3 eV: ●, C_6H_6 and ○, C_6F_6; (*c*) C_6H_6 at ●, 4.94 eV and C_6F_6 at ○, 5.0 eV; and (*d*) at 10 eV ●, C_6H_6 and ○, C_6F_6.

60°–80° with forward angle minima near 30°. At 3.0 eV (figure 8(*b*)) the DCS for C_6F_6 is almost identical to that for 1.5 eV with the exception of the most forward scattering angles, where the magnitude has decreased. The DCS for C_6H_6 is similar at the most forward scattering angles, but differs dramatically at larger angles with the most prominent difference being the local minimum that is seen at around 30°.

Figure 8(*c*) show the comparison of the DCS for C_6H_6 at 4.94 eV with C_6F_6 at 5 eV. For this case, the DCS for C_6H_6 is larger in magnitude for the entire measured angular range. This is most likely due to the presence of the $^2B_{2g}$ resonance in C_6H_6 at this energy which is also seen to enhance the magnitude of the total cross section considerably. At 10 eV (figure 8(*d*)), the shape and the magnitude of DCS for both molecules are similar, especially for forward scattering angles. For larger angles (65°–130°), the DCS for C_6F_6 does not show the structure seen in the DCS for C_6H_6. At 15, 20 and 30 eV (not shown), both molecules show remarkable similarities at low angles (below 40°) in terms of the magnitude and shape of the differential cross section. At higher scattering angles, the cross sections show similar structures, but the magnitude of the cross sections for C_6F_6 are generally 1.5–2 times larger.

There is a general similarity in both the shapes and magnitudes of the total cross sections for C_6H_6 and C_6F_6, although we note that the peak cross section for C_6F_6 is shifted towards higher electron energies and the main maximum in the cross section is much broader. The most prominent features of the elastic integral cross sections for both target molecules are their relatively high magnitudes throughout the experimental energy range, always exceeding 18.5 Å^2. One significant difference between the two molecules is that the total inelastic cross section (the difference between the present total elastic cross section and the grand total cross section) is significantly larger for energies above about 20 eV for C_6F_6 than for C_6H_6. A substantial amount of this large difference is most probably due to ionization.

4. Conclusions

Absolute elastic differential cross sections for C_6H_6 have been measured at 13 incident electron energies between 1.1 and 40 eV, and for C_6F_6 at 10 energies between 1.5 and 100 eV. The present measurements provide an encouraging picture of the level of agreement between theory and experiment for electron scattering from both target molecules, particularly for energies above 5 eV. The presence and nature of low-energy negative-ion resonances in C_6H_6 at 1.15, 4.9 and around 8–9 eV were confirmed, but higher-lying resonances predicted around 20 eV were not observed. The present total elastic cross sections agree well with their respective theoretical calculations, especially in energy regions away from the influence of the strong negative-ion resonances.

Acknowledgments

HC gratefully acknowledges the award of an Australian Research Council (ARC) International Visiting Fellowship and RJG an ARC Postdoctoral Fellowship. LJU is grateful to the Australian Government for the provision of a Postgraduate Research Scholarship. We thank Professors Franco Gianturco, Robert Lucchese, Alexandra Natalense and Carl Winstead for the provision of tabulated cross section values, in some cases prior to publication. SJB is delighted to acknowledge initial discussions with Paul Burrow who convinced him of the need for such a study in benzene. It is, as always, a pleasure to acknowledge the expert assistance of the technical staff of the Atomic and Molecular Physics Laboratories, particularly Kevin Roberts and Steve Battisson.

References

Allan M 1989 *J. Electron Spectrosc. Relat. Phenom.* **48** 219
Azria R and Schulz G J 1975 *J. Chem. Phys.* **62** 573
Bardsley J N and Read F H 1968 *Chem. Phys. Lett.* **2** 333
Bettega M H F, Winstead C and McKoy V 2000 *J. Chem. Phys.* **112** 8806
Boesten L and Tanaka H 1992 *At. Data Nucl. Data Tables* **52** 25
Brunger M J, Buckman S J, Allen L J, McCarthy I E and Ratnavelu K 1992 *J. Phys. B: At. Mol. Opt. Phys.* **25** 1823
Brunger M J, Buckman S J and Newman D S 1990 *Aust. J. Phys.* **43** 665
Brunt J N H, King G C and Read F H 1977 *J. Phys. B: At. Mol. Phys.* **10** 1289
Burrow P D, Michejda J A and Jordan K D 1987 *J. Chem. Phys.* **86** 9
Christophorou L G and Datskos P G 1995 *Int. J. Mass Spectrom. Ion Proc.* **149/150** 59
Gallup G A 1993 *J. Chem. Phys.* **99** 827
Gianturco F A and Lucchese R R 1998 *J. Chem. Phys.* **108** 6144
——1998 Private communication
Gulley R J, Alle D T, Brennan M J, Brunger M J and Buckman S J 1994 *J. Phys. B: At. Mol. Opt. Phys.* **27** 2593
Gulley R J and Buckman S J 1999 *J. Phys. B: At. Mol. Opt. Phys.* **32** L405
Gulley R J, Lunt S L, Ziesel J-P and Field D 1998 *J. Phys. B: At. Mol. Opt. Phys.* **31** 2735
Holst W and Holtsmark J 1931 *K. Norsk. Vidensk. Selsk.* **4** 89
Karwasz G, Brusa R, Piazza A and Zecca A 1999 *Phys. Rev.* A **59** 1341
Kasperski G, Mozejko P and Szmytkowski C 1997 *Z. Phys.* D **42** 187
Kitajima M, Sakamoto Y, Gulley R J, Hoshino M, Gibson J C, Tanaka H and Buckman S J 2000 *J. Phys. B: At. Mol. Opt. Phys.* **33** 1687
Marawar R W, Walter C W, Smith K A and Dunning F B 1988 *J. Chem. Phys.* **88** 2853
Mather D and Hasted J B 1976 *J. Phys. B: At. Mol. Phys.* **9** L31
Mozejko P, Kasperski G, Szmytkowski C, Karwasz G P, Brusa R S and Zecca A 1996 *Chem. Phys. Lett.* **257** 309
Natalense A P P, Bettega M H F, Ferreira L G and Lima M A P 1999 *Phys. Rev.* A **59** 879
Natalense A P P and Lucchese R R 2001 *J. Chem. Phys.* at press
Nenner I and Schulz G J 1975 *J. Chem. Phys.* **62** 1747
Nesbet R K 1979 *Phys. Rev.* A **20** 58
Nickel J C, Zetner P W, Shen G and Trajmar S 1989 *J. Phys. E: Sci. Instrum.* **22** 730
Rohr K 1977 *J. Phys. B: At. Mol. Phys.* **10** 2215
Sanche L and Schulz G J 1973 *J. Chem. Phys.* **58** 479
Srivastava S K, Chutjian A and Trajmar S 1975 *J. Chem. Phys.* **63** 2659
Sueoka O 1988 *J. Phys. B: At. Mol. Opt. Phys.* **21** L631
Tanaka H, Boesten L, Matsunaga D and Kudo T 1988 *J. Phys. B: At. Mol. Opt. Phys.* **21** 255
Tanaka H, Masai T, Kimura M, Nishimura T and Itikawa Y 1997 *Phys. Rev.* A **56** R3338
Tanaka H, Tachibana Y, Kitajima M, Sueoka O, Takaki H, Hamada A and Kimura M 1999 *Phys. Rev.* A **59** 2006
Weik F and Illenberger E 1995 *J. Chem. Phys.* **103** 1406
Winstead C, McKoy V and Bettega M H F 1999 *Bull. Am. Phys. Soc.* **44**
——1999 Private communication
Wong S F and Schulz G J 1975 *Phys. Rev. Lett.* **35** 1429